

ERDC SR-22-2

Engineer Research and  
Development Center



**US Army Corps  
of Engineers®**  
Engineer Research and  
Development Center



*Acoustic Wind Noise Modeling for Complex Environments*

# **A Tutorial on the Rapid Distortion Theory Model for Unidirectional, Plane Shearing of Homogeneous Turbulence**

Carl R. Hart and Gregory W. Lyons

July 2022

**The U.S. Army Engineer Research and Development Center (ERDC)** solves the nation's toughest engineering and environmental challenges. ERDC develops innovative solutions in civil and military engineering, geospatial sciences, water resources, and environmental sciences for the Army, the Department of Defense, civilian agencies, and our nation's public good. Find out more at [www.erdclibrary.on.worldcat.org/discovery](http://www.erdclibrary.on.worldcat.org/discovery).

To search for other technical reports published by ERDC, visit the ERDC online library at <http://www.erdclibrary.on.worldcat.org/discovery>.

# **A Tutorial on the Rapid Distortion Theory Model for Unidirectional, Plane Shearing of Homogeneous Turbulence**

Carl R. Hart

*U.S. Army Engineer Research and Development Center (ERDC)  
Cold Regions Research and Engineering Laboratory (CRREL)  
72 Lyme Road  
Hanover, NH 03755-1290*

Gregory W. Lyons

*U.S. Army Engineer Research and Development Center (ERDC)  
Information Technology Laboratory (ITL)  
3909 Halls Ferry Road  
Vicksburg, MS 39180*

Final Report

Approved for public release; distribution is unlimited.

Prepared for Headquarters, U.S. Army Corps of Engineers  
Washington, DC 20314-1000

Under PE 611102 / Project AB2 / Task A1040

## Abstract

The theory of near-surface atmospheric wind noise is largely predicated on assuming turbulence is homogeneous and isotropic. For high turbulent wavenumbers, this is a fairly reasonable approximation, though it can introduce non-negligible errors in shear flows. Recent near-surface measurements of atmospheric turbulence suggest that anisotropic turbulence can be adequately modeled by rapid-distortion theory (RDT), which can serve as a natural extension of wind noise theory. Here, a solution for the RDT equations of unidirectional plane shearing of homogeneous turbulence is reproduced. It is assumed that the time-varying velocity spectral tensor can be made stationary by substituting an eddy-lifetime parameter in place of time. General and particular RDT evolution equations for stochastic increments are derived in detail. Analytical solutions for the RDT evolution equation, with and without an effective eddy viscosity, are given. An alternative expression for the eddy-lifetime parameter is shown. The turbulence kinetic energy budget is examined for RDT. Predictions by RDT are shown for velocity (co)variances, one-dimensional streamwise spectra, length scales, and the second invariant of the anisotropy tensor of the moments of velocity. The RDT prediction of the second invariant for the velocity anisotropy tensor is shown to agree better with direct numerical simulations than previously reported.

# Contents

<b>Abstract</b> .....	<b>ii</b>
<b>Figures</b> .....	<b>iv</b>
<b>Preface</b> .....	<b>v</b>
<b>1 Introduction</b> .....	<b>1</b>
<b>2 The Stochastic Fourier-Stieltjes Integral of Turbulent Velocity</b> .....	<b>3</b>
<b>3 Evolution Equation for Stochastic Increments by Rapid Distortion Theory</b> .....	<b>5</b>
Effective eddy viscosity .....	9
<b>4 Analytical Solution to the Uniform Shear Rapid Distortion Equation</b> .....	<b>10</b>
4.1 Effective eddy viscosity factor .....	14
4.2 Mass conservation .....	15
<b>5 Eddy-Lifetime Parameter</b> .....	<b>17</b>
<b>6 Turbulence Kinetic Energy Budget</b> .....	<b>20</b>
<b>7 Shear-Distorted Velocity Covariances, Spectra, and Length Scales</b> .....	<b>23</b>
Second Invariant for the Velocity Anisotropy Tensor .....	29
<b>8 Conclusion</b> .....	<b>32</b>
<b>References</b> .....	<b>33</b>
<b>Report Documentation Page</b> .....	<b>35</b>

# Figures

## Figures

Figure 1. Rapid distortion theory integrated TKE budget terms as a function of nondimensional time $\beta$ .....	22
Figure 2. Normalized velocity (co)variances as a function of nondimensional time $\beta$ .....	25
Figure 3. Normalized premultiplied one-dimensional spectra as a function of nondimensional streamwise wavenumber $n_1$ . Nondimensional time $\beta = 1$ .....	25
Figure 4. Normalized premultiplied one-dimensional spectra as a function of nondimensional streamwise wavenumber $n_1$ . Nondimensional time $\beta = 1$ . Both axes are logarithmically scaled.....	26
Figure 5. Normalized length scales as a function of nondimensional time $\beta$ .....	27
Figure 6. Normalized premultiplied one-dimensional spectra as a function of nondimensional streamwise wavenumber $n_1$ . Shear anisotropy parameter $\Upsilon = 3$ .....	28
Figure 7. Normalized premultiplied one-dimensional spectra as a function of nondimensional streamwise wavenumber $n_1$ . Shear anisotropy parameter $\Upsilon$ varies according to the legend.....	29
Figure 8. Second invariant for the velocity anisotropy tensor as a function of nondimensional time $\beta$ ; solid line: from Equation (44), dashed line: from Equation (42), filled circles: DNS results from Lee et al. (1990).....	30
Figure 9. Moments of velocity $b_{ij}$ as a function of nondimensional time $\beta$ ; symbols: DNS results from Lee et al. (1990).....	31

## Preface

This study was conducted for the U.S. Army Corps of Engineers under Project 611102/AB2/A1040, “Acoustic Wind Noise Modeling for Complex Environments.”

The work was performed by the Signature Physics Branch of the Research and Engineering Division, U.S. Army Engineer Research and Development Center (ERDC), Cold Regions Research and Engineering Laboratory (CRREL). At the time of publication, Dr. Steven E. Peckham was Acting Branch Chief; and Dr. George Calfas was Division Chief. The Acting Deputy Director of ERDC-CRREL was Mr. Bryan E. Baker, and the Director was Dr. Joseph L. Corriveau.

COL Teresa A. Schlosser was Commander of ERDC, and Dr. David W. Pittman was the Director.

# 1 Introduction

The theory of near-surface atmospheric wind noise—that is, static and stagnation interaction pressure fluctuations—is largely predicated on assuming turbulence is homogeneous and isotropic (Raspet et al. 2008). For high turbulent wavenumbers this is a fairly reasonable approximation, though it can introduce non-negligible errors in shear flows (Wyngaard 2010, pp. 326, 327). Later work considered an anisotropic turbulence model, Kraichnan's mirror flow model (Kraichnan 1956), for static (shear-turbulence) pressure fluctuations, which is prominent at low turbulent wavenumbers (Yu et al. 2011). Recent near-surface measurements of atmospheric turbulence suggest that anisotropic turbulence can be adequately modeled by rapid-distortion theory (RDT) (Chougule et al. 2017, 2018), which can serve as a natural extension of wind noise theory. These models for anisotropic turbulence consider the presence of a temperature gradient and plane shearing of homogeneous turbulence.

Unidirectional, plane shearing of homogeneous turbulence is a fundamental problem in turbulence research. Under the premise of “weak turbulence” (Townsend 1976, p. 81), Townsend (1970) presented the first analytical solutions for the Fourier series expansion of turbulent velocity components. These solutions effectively apply to the RDT equations by neglecting terms containing an “effective eddy viscosity.” Hunt and Carruthers (1990) notes that features of turbulent shear flows over boundary layers can be described by RDT models for homogeneous turbulence in a uniform shear. In their review, considerable discussion was given to RDT predictions of covariances, comparisons to direct numerical simulations (DNS), and spectra. It was emphasized that the main result of RDT is to show that linear distortion effects of the mean shear dominate nonlinear interactions in the high-wavenumber range.

The physical assumptions inherent to RDT are discussed at length by Cambon and Scott (1999). In particular the time scale of distortion by the mean flow is small compared to turbulent evolution in the absence of distortion. In other words, linearization of the Navier-Stokes equation implies, for large scales, the characteristic root-mean-square fluctuating velocity is much less than the product of mean strain (shear) and a correlation length scale. As a consequence, interaction of turbulence with

itself, including the cascade process, is ignored. Furthermore, initially homogeneous turbulence remains homogeneous if the flow is uniformly sheared.

Here, a solution for the RDT equations of unidirectional plane shearing of homogeneous turbulence is reproduced. Particular attention is given to the presentation by Mann (1994), in which it is assumed that the time-varying velocity spectral tensor can be made stationary by substituting an eddy-lifetime parameter in place of time. Section 2 reviews the stochastic Fourier-Stieltjes formalism for representing turbulent velocity fields. Section 3 outlines general and particular RDT evolution equations for stochastic increments. Section 4 provides the analytical solution for both the RDT evolution equation and for the case where an effective eddy viscosity is retained. Mass conservation is noted for the analytical solution. Section 5 derives the eddy-lifetime parameter. An alternative expression for the eddy-lifetime parameter is given. Section 6 examines the turbulence kinetic energy budget associated with the uniform-shear RDT equation. Section 7 discusses the consequences of the RDT solution with respect to velocity (co)variances, one-dimensional streamwise spectra, length scales, and the second invariant of the anisotropy tensor of the moments of velocity. The RDT prediction of the second invariant for the velocity anisotropy tensor is shown to agree better with direct numerical simulations than previously reported.

## 2 The Stochastic Fourier-Stieltjes Integral of Turbulent Velocity

By Reynolds decomposition the turbulent velocity field,  $\tilde{u}_i(\mathbf{x}; t) = U_i(\mathbf{x}; t) + u_i(\mathbf{x}; t)$ , is a linear sum of a mean velocity field and fluctuating velocity field, and  $u_i = (u_1, u_2, u_3)$ . Assume the fluctuating field is statistically homogeneous in space  $\mathbf{x} = (x_1, x_2, x_3)$ , and nonstationary in time,  $t$ . In this case time is represented as a parameter. The fluctuating velocity field is a stochastic process that is neither integrable nor periodic. As a consequence, Fourier analysis is not formally applicable for fluctuating velocity  $u_i$ . Instead, a stochastic Fourier-Stieltjes integral represents the fluctuating velocity field through another stochastic process,  $Z_i(\mathbf{k}; t)$  (Wyngaard 2010, pp. 332–336),

$$u_i(\mathbf{x}; t) = \iiint_{-\infty}^{\infty} e^{i\mathbf{k}\cdot\mathbf{x}} dZ_i(\mathbf{k}; t), \quad (1)$$

where  $\mathbf{k} = (k_1, k_2, k_3)$  is the turbulent wavenumber vector,  $dZ_i(\mathbf{k}; t)$  is a difference or increment in  $Z_i$ , and the integral is over all wavenumbers. The differences  $dZ_i(\mathbf{k}; t)$  may be considered as complex amplitudes of the Fourier modes for turbulent wavenumber.

Important properties of the Fourier-Stieltjes integral include orthogonality of stochastic increments and its relationship to the velocity spectral tensor. The stochastic differences of  $Z_i$  are complex valued and its components are orthogonal in wavenumber space (Batchelor 1953, pp. 31–33),

$$\langle dZ_i^*(\mathbf{k}; t) dZ_j(\mathbf{k}'; t) \rangle = \begin{cases} 0, & \mathbf{k} \neq \mathbf{k}' \\ \phi_{ij}(\mathbf{k}; t) d^3\mathbf{k}, & \mathbf{k} = \mathbf{k}' \end{cases} \quad (2)$$

where  $\langle \cdot \rangle$  is the ensemble average operator,  $d^3\mathbf{k} = dk_1 dk_2 dk_3$ , and  $\phi_{ij}(\mathbf{k}; t)$  is the velocity spectral tensor. This quantifies the spatial scale and intensity of turbulence (Glegg and Devenport 2017, Sec. 8.4.3). The spatial cross-correlation of turbulent velocity components is related to the velocity spectral tensor through a three-dimensional Fourier transform,

$$R_{ij}(\mathbf{r}; t) = \langle u_i(\mathbf{x}; t) u_j(\mathbf{x} + \mathbf{r}; t) \rangle,$$

$$\begin{aligned}
&= \iiint_{-\infty}^{\infty} e^{-i\mathbf{k}\cdot\mathbf{x}+ik'(\mathbf{x}+\mathbf{r})} \langle dZ_i^*(\mathbf{k};t)dZ_j(\mathbf{k}';t) \rangle, \\
&= \iiint_{-\infty}^{\infty} e^{i\mathbf{k}\cdot\mathbf{r}} \phi_{ij}(\mathbf{k};t) d^3\mathbf{k},
\end{aligned}$$

where the complex conjugate of  $u_i$ , being equal to itself, is used above. The inverse Fourier transform of the spatial cross-correlation gives the velocity spectral tensor,

$$\phi_{ij}(\mathbf{k};t) = \frac{1}{(2\pi)^3} \iiint_{-\infty}^{\infty} e^{-i\mathbf{k}\cdot\mathbf{r}} R_{ij}(\mathbf{r};t) d^3\mathbf{r} .$$

By the continuity equation,  $\partial u_i / \partial x_i = 0$ , it can be shown that stochastic increments are also orthogonal to the turbulent wavenumber vector,

$$k_i dZ_i(\mathbf{k};t) = 0 ,$$

where it is understood that Einstein notation is used such that repeated indices are summed over—that is,  $k_i dZ_i = k_1 dZ_1 + k_2 dZ_2 + k_3 dZ_3 = 0$ . By way of Equations (1), (2), and the continuity equation, the following properties hold for the spatial cross-correlation and velocity spectral tensor:

$$\begin{aligned}
R_{ij}(\mathbf{r};t) &= R_{ji}(-\mathbf{r};t), \\
\phi_{ij}(\mathbf{k};t) &= \phi_{ji}(-\mathbf{k};t), \\
\phi_{ij}(\mathbf{k};t) &= \phi_{ji}^*(\mathbf{k};t), \\
k_i \phi_{ij}(\mathbf{k};t) &= k_j \phi_{ij}(\mathbf{k};t) = 0.
\end{aligned}$$

### 3 Evolution Equation for Stochastic Increments by Rapid Distortion Theory

A general evolution equation for stochastic increments, associated with turbulent velocity, follows from application of rapid distortion theory to the Navier-Stokes equation. Neglecting gravity and the rotation of the Earth, for an incompressible, constant density fluid, the Navier-Stokes equation is

$$\frac{\partial \tilde{u}_i}{\partial t} + \tilde{u}_j \frac{\partial \tilde{u}_i}{\partial x_j} = -\frac{1}{\rho} \frac{\partial \tilde{p}}{\partial x_i} + \nu \frac{\partial^2 \tilde{u}_i}{\partial x_j^2},$$

Where  $\tilde{p}$  is fluid pressure,  $\rho$  is fluid density, and  $\nu$  is kinematic viscosity. Each dependent variable,  $\tilde{u}_i$  and  $\tilde{p}$ , are functions of position and time. The Navier-Stokes equation expresses conservation of momentum for fluid flow. Conservation of mass is expressed by the continuity equation

$$\frac{\partial \tilde{u}_i}{\partial x_i} = 0. \quad (4)$$

Since the ensemble average is a linear operator—that is, it commutes with the gradient (Wyngaard 2010, p. 30), application to Equation (4) gives  $\partial U_i / \partial x_i = 0$ . Take the divergence of Equation (3) and consider the continuity equation

$$\begin{aligned} \frac{\partial}{\partial t} \frac{\partial \tilde{u}_i}{\partial x_i} + \frac{\partial \tilde{u}_j}{\partial x_i} \frac{\partial \tilde{u}_i}{\partial x_j} + \tilde{u}_j \frac{\partial^2 \tilde{u}_i}{\partial x_j \partial x_i} &= -\frac{1}{\rho} \frac{\partial^2 \tilde{p}}{\partial x_i^2} + \nu \frac{\partial^2}{\partial x_j^2} \frac{\partial \tilde{u}_i}{\partial x_i}, \\ \frac{\partial \tilde{u}_j}{\partial x_i} \frac{\partial \tilde{u}_i}{\partial x_j} &= -\frac{1}{\rho} \frac{\partial^2 \tilde{p}}{\partial x_i^2}. \end{aligned}$$

Rearrange right- and left-hand sides,

$$\begin{aligned} -\frac{1}{\rho} \frac{\partial^2 \tilde{p}}{\partial x_i^2} &= \frac{\partial^2}{\partial x_i \partial x_j} (\tilde{u}_i \tilde{u}_j), \\ &= \frac{\partial^2}{\partial x_i \partial x_j} (U_i U_j + u_j U_i + u_i U_j + u_i u_j). \end{aligned}$$

Take the ensemble average of both sides,

$$-\frac{1}{\rho} \frac{\partial^2 P}{\partial x_i^2} = \frac{\partial^2}{\partial x_i \partial x_j} (U_i U_j + \langle u_i u_j \rangle),$$

and subtract this from the earlier expression,

$$\begin{aligned} -\frac{1}{\rho} \frac{\partial^2 p}{\partial x_i^2} &= \frac{\partial^2}{\partial x_i \partial x_j} (u_j U_i + u_i U_j + u_i u_j - \langle u_i u_j \rangle), \\ &= \frac{\partial u_j}{\partial x_i} \frac{\partial U_i}{\partial x_j} + \frac{\partial u_i}{\partial x_j} \frac{\partial U_j}{\partial x_i} + \frac{\partial^2}{\partial x_i \partial x_j} (u_i u_j - \langle u_i u_j \rangle). \end{aligned}$$

Rearranging indices gives the fluctuating pressure Poisson equation,

$$-\frac{1}{\rho} \frac{\partial^2 p}{\partial x_i^2} = 2 \frac{\partial U_j}{\partial x_i} \frac{\partial u_i}{\partial x_j} + \frac{\partial^2}{\partial x_i \partial x_j} (u_i u_j - \langle u_i u_j \rangle). \quad (5)$$

Rapid distortion theory postulates that in the limit of rapid distortion, the first term on the right-hand side of Equation (5) is much larger than the remaining terms,

$$-\frac{1}{\rho} \frac{\partial^2 p}{\partial x_i^2} = 2 \frac{\partial U_j}{\partial x_i} \frac{\partial u_i}{\partial x_j}. \quad (6)$$

In other words, linear distortion effects of the mean shear dominate nonlinear interactions (Hunt and Carruthers 1990). Returning to Equation (3), neglecting viscosity and subtracting the ensemble average gives the fluctuating pressure gradient

$$-\frac{1}{\rho} \frac{\partial p}{\partial x_i} = \frac{\partial u_i}{\partial t} + U_j \frac{\partial u_i}{\partial x_j} + u_j \frac{\partial U_i}{\partial x_j} + \frac{\partial}{\partial x_j} (u_i u_j - \langle u_i u_j \rangle). \quad (7)$$

In rapid distortion theory, second-order fluctuations are neglected in Equation (7), resulting in

$$-\frac{1}{\rho} \frac{\partial p}{\partial x_i} = \frac{\partial u_i}{\partial t} + U_j \frac{\partial u_i}{\partial x_j} + u_j \frac{\partial U_i}{\partial x_j}. \quad (8)$$

Defining the average material derivative as

$$\frac{\overline{D}}{Dt} = \frac{\partial}{\partial t} + U_j \frac{\partial}{\partial x_j}$$

provides for a succinct expression of the fluctuating linearized Navier-Stokes equation:

$$-\frac{1}{\rho} \frac{\partial p}{\partial x_i} = \frac{\overline{D}u_i}{Dt} + u_j \frac{\partial U_i}{\partial x_j}. \quad (9)$$

Consider a uniform mean shear in the flow:

$$U_j = x_k \frac{\partial U_j}{\partial x_k}. \quad (10)$$

This shear distorts turbulent wavenumber vectors according to the following ordinary differential equation (Townsend 1976, Eq. (3.2.8)):

$$\frac{dk_k}{dt} = -k_j \frac{\partial U_j}{\partial x_k}. \quad (11)$$

The spatial scales of turbulence distort and rotate according to Equation (11) as a result of flow being solenoidal (velocity and mean velocity have zero divergence) (Townsend 1976, p. 47). The Fourier-Stieltjes integral of the average material derivative of fluctuating velocity is

$$\begin{aligned} \frac{\overline{D}u_i}{Dt} &= \left( \frac{\partial}{\partial t} + U_j \frac{\partial}{\partial x_j} \right) u_i(\mathbf{x}; t), \\ &= \iiint_{-\infty}^{\infty} e^{i\mathbf{k}\cdot\mathbf{x}} \left[ \left( \frac{\partial}{\partial t} + ik_j U_j \right) dZ_i(\mathbf{k}; t) \right], \\ &= \iiint_{-\infty}^{\infty} e^{i\mathbf{k}\cdot\mathbf{x}} \left[ \left( \frac{\partial}{\partial t} + \frac{dk_k}{dt} \frac{\partial}{\partial k_k} \right) dZ_i(\mathbf{k}; t) \right], \end{aligned}$$

which is proved by recognizing  $\partial k_j / \partial k_k = 0$  when indices  $k \neq j$ , and by continuity  $\partial U_j / \partial x_k = 0$  when indices  $k = j$ . A shorthand for the operator in the Fourier-Stieltjes integral is defined as

$$\frac{\tilde{D}}{\tilde{D}t} = \frac{\partial}{\partial t} + \frac{dk_k}{dt} \frac{\partial}{\partial k_k},$$

which can be thought of as an average material derivative in turbulent wavenumber space.

A general evolution equation for stochastic increments follows from Equations (6) and (9). Consider the following Fourier-Stieltjes integral for fluctuating pressure,

$$p(\mathbf{x}; t) = \iiint_{-\infty}^{\infty} e^{i\mathbf{k}\cdot\mathbf{x}} dY(\mathbf{k}; t) .$$

Converting Equation (6) to its Fourier-Stieltjes representation and equating stochastic increments of fluctuating pressure to fluctuating velocity gives

$$\frac{k^2}{\rho} dY(\mathbf{k}; t) = i2k_j \frac{\partial U_j}{\partial x_i} dZ_i(\mathbf{k}; t) .$$

Multiplying by  $-ik_i$  and dividing by  $k^2$  results in

$$\frac{-ik_i}{\rho} dY(\mathbf{k}; t) = 2 \frac{k_i k_j}{k^2} \frac{\partial U_j}{\partial x_i} dZ_i(\mathbf{k}; t) .$$

The Fourier-Stieltjes integral of Equation (9) gives the following equality:

$$\frac{-ik_i}{\rho} dY(\mathbf{k}; t) = \frac{\tilde{D}}{\tilde{D}t} dZ_i(\mathbf{k}; t) + \frac{\partial U_i}{\partial x_j} dZ_j(\mathbf{k}; t) .$$

Combining these two expressions gives the evolution equation for stochastic increments of fluctuating velocity:

$$\frac{\tilde{D}}{\tilde{D}t} dZ_i(\mathbf{k}; t) = 2 \frac{k_i k_j}{k^2} \frac{\partial U_j}{\partial x_k} dZ_k(\mathbf{k}; t) - \frac{\partial U_i}{\partial x_j} dZ_j(\mathbf{k}; t) . \quad (12)$$

Equation (12) is similar to Equation (3.10.3) of (Townsend 1976), except that continuous wavenumbers are considered here, as opposed to discrete wavenumbers, and rather than representing fluctuating velocity as a

Fourier series, here it is represented as stochastic increments via the Fourier-Stieltjes integral representation.

Consider streamwise coordinates such that the only nonzero term in mean shear is  $\partial U_1 / \partial x_3$ . Under this condition, the uniform shear rapid distortion equation is (Mann 1994, Eq. (3.11))

$$\frac{\tilde{D}}{\tilde{D}t} dZ_i(\mathbf{k}; t) = \frac{\partial U_1}{\partial x_3} \left( 2 \frac{k_i k_1}{k^2} - \delta_{i1} \right) dZ_3(\mathbf{k}; t). \quad (13)$$

Furthermore, the solution to Equation (11), given initial conditions  $\mathbf{k}(t=0) = \mathbf{k}_0 = (k_1, k_2, k_{30})$ , is simply (Townsend 1976, p. 83)

$$\begin{aligned} \mathbf{k} &= (k_1, k_2, k_3) \\ &= (k_1, k_2, k_{30} - k_1 \beta), \end{aligned} \quad (14)$$

where  $\beta = (\partial U_1 / \partial x_3) t$  is a nondimensional time. Note, the average material derivative in turbulent wavenumber space is appropriately interpreted as a total time derivative. Therefore, Equation (13) can be interpreted as a system of ordinary differential equations:

$$\frac{d}{dt} dZ_i(\mathbf{k}; t) = \frac{\partial U_1}{\partial x_3} \left( 2 \frac{k_i k_1}{k^2} - \delta_{i1} \right) dZ_3(\mathbf{k}; t). \quad (15)$$

### Effective eddy viscosity

In discussing an evolution equation for Fourier components of fluctuating velocity (i.e., stochastic increments  $dZ_i$ ), Townsend (1976, p. 73) remarks that “interactions between pairs of Fourier components are negligible, if both contribute to the larger eddies, and that interaction between these components and components of larger wavenumber (smaller eddies) has the general effect of a viscous damping.” This effect is introduced into the stochastic increment evolution equation by way of an effective eddy viscosity  $\nu_i$ :

$$\frac{d}{dt} dZ_i(\mathbf{k}; t) = -\nu_i k^2 dZ_i(\mathbf{k}; t) + \frac{\partial U_1}{\partial x_3} \left( 2 \frac{k_i k_1}{k^2} - \delta_{i1} \right) dZ_3(\mathbf{k}; t), \quad (16)$$

which accounts for viscous damping by smaller eddies.

## 4 Analytical Solution to the Uniform Shear Rapid Distortion Equation

The uniform shear rapid distortion equation is a system of first-order ordinary differential equations that are analytically soluble. Consider first the third component of the stochastic increment,

$$\frac{d}{dt} dZ_3(\mathbf{k}; t) = 2k_1 \frac{\partial U_1}{\partial x_3} \frac{k_3}{k^2} dZ_3(\mathbf{k}; t).$$

A detailed solution for this equation will be given, and only critical details will be described for the other components. The following indefinite integral will be of use:

$$\begin{aligned} \int \frac{k_3}{k^2} dk_3 &= \frac{1}{k_1^2 + k_2^2} \int \frac{k_3}{1 + k_3^2 / (k_1^2 + k_2^2)} dk_3, \\ &= \int \tan \theta d\theta, \\ &= - \int \frac{1}{x} dx, \\ &= \ln \left( \frac{k}{\sqrt{k_1^2 + k_2^2}} \right) + c, \end{aligned}$$

where  $c$  is a constant of integration, a substitution of  $\tan \theta = k_3 / \sqrt{k_1^2 + k_2^2}$ , and  $dk_3 = \sqrt{k_1^2 + k_2^2} (1 + \tan^2 \theta) d\theta$  is made after the first line, followed by a substitution of  $x = \cos \theta$  and  $dx = -\sin \theta d\theta$ . For  $dZ_3$  the method of solution is by separation of variables. Integrating from time zero to  $t$ ,

$$\begin{aligned} \int_0^t \frac{d[dZ_3(\mathbf{k}; t')]}{dZ_3(\mathbf{k}; t')} &= 2k_1 \frac{\partial U_1}{\partial x_3} \int_0^t \frac{k_3}{k^2} dt', \\ \ln \left( \frac{dZ_3(\mathbf{k}; t)}{dZ_3(\mathbf{k}_0; 0)} \right) &= -2 \int_{k_{30}}^{k_3} \frac{k_3'}{k_2} dk_3', \\ &= \ln \left( \frac{k_0^2}{k^2} \right), \end{aligned}$$

where the substitution  $k_3' = k_{30} - k_1(\partial U_1 / \partial x_3)t'$  and  $dk_3' = -k_1(\partial U_1 / \partial x_3)dt'$  follows the first line. Hence,

$$dZ_3(\mathbf{k}; t) = \frac{k_0^2}{k^2} dZ_3(\mathbf{k}_0; 0). \quad (17)$$

Substituting Equation (17) back into Equation (15) serves as a check.

Since  $dZ_3$  is known, solving for  $dZ_2$  follows along the same lines. In particular,

$$\frac{d}{dt} dZ_2(\mathbf{k}; t) = 2k_1 \frac{\partial U_1}{\partial x_3} \frac{k_2 k_0^2}{k^4} dZ_3(\mathbf{k}_0; 0),$$

which as before is solved by separation of variables and integrating from time zero to  $t$ . The following indefinite integral is required:

$$\begin{aligned} \int \frac{1}{k^4} dk_3 &= \frac{1}{(k_1^2 + k_2^2)^2} \int \frac{1}{[1 + k_3^2 / (k_1^2 + k_2^2)]^2} dk_3, \\ &= \frac{1}{(k_1^2 + k_2^2)^{3/2}} \int \cos^2 \theta d\theta, \\ &= \frac{k_3}{2(k_1^2 + k_2^2)k^2} + \frac{1}{2(k_1^2 + k_2^2)^{3/2}} \tan^{-1} \left( \frac{k_3}{\sqrt{k_1^2 + k_2^2}} \right) + c, \end{aligned}$$

where the substitution  $\tan \theta = k_3 / \sqrt{k_1^2 + k_2^2}$  is used as before, and the indefinite integral for  $\cos^2 \theta$  follows from use of the double angle formula—that is,  $\cos^2 \theta = [1 + \cos(2\theta)] / 2$ . The solution for  $dZ_2$  is

$$\begin{aligned} dZ_2(\mathbf{k}; t) &= dZ_2(\mathbf{k}_0; 0) + \left( \frac{k_2(k_{30}k^2 - k_3k_0^2)}{(k_1^2 + k_2^2)k^2} + \frac{k_2k_0^2}{(k_1^2 + k_2^2)^{3/2}} \right. \\ &\quad \left. \times \left[ \tan^{-1} \left( \frac{k_{30}}{\sqrt{k_1^2 + k_2^2}} \right) - \tan^{-1} \left( \frac{k_3}{\sqrt{k_1^2 + k_2^2}} \right) \right] \right) dZ_3(\mathbf{k}_0; 0) \end{aligned} \quad (18)$$

The solution for  $dZ_1$  is nearly identical to  $dZ_2$ , except one additional indefinite integral is required. This arises from a second term in the ordinary differential equation:

$$\frac{d}{dt} dZ_1(\mathbf{k}; t) = k_1 \frac{\partial U_1}{\partial x_3} \left( \frac{2k_1 k_0^2}{k^4} - \frac{k_0^2}{k_1 k^2} \right) dZ_3(\mathbf{k}_0; 0).$$

The required indefinite integral is

$$\begin{aligned} \int \frac{1}{k^2} dk_3 &= \frac{1}{k_1^2 + k_2^2} \int \frac{1}{1 + k_3^2 / (k_1^2 + k_2^2)} dk_3, \\ &= \frac{1}{\sqrt{k_1^2 + k_2^2}} \int d\theta, \\ &= \frac{1}{\sqrt{k_1^2 + k_2^2}} \tan^{-1} \left( \frac{k_3}{\sqrt{k_1^2 + k_2^2}} \right) + c. \end{aligned}$$

The solution for  $dZ_1$  is

$$\begin{aligned} dZ_1(\mathbf{k}; t) &= dZ_1(\mathbf{k}_0; 0) + \left( \frac{k_1(k_{30}k^2 - k_3k_0^2)}{(k_1^2 + k_2^2)k^2} - \frac{k_2^2 k_0^2}{k_1(k_1^2 + k_2^2)^{3/2}} \right. \\ &\quad \left. \times \left[ \tan^{-1} \left( \frac{k_{30}}{\sqrt{k_1^2 + k_2^2}} \right) - \tan^{-1} \left( \frac{k_3}{\sqrt{k_1^2 + k_2^2}} \right) \right] \right) dZ_3(\mathbf{k}_0; 0). \end{aligned} \quad (19)$$

Equations (17–19) are equivalent in form to solutions by Hunt and Carruthers (1990), in which they cite Townsend (1970). The inverse tangent terms in the solutions can be combined by the identity  $\tan^{-1}x - \tan^{-1}y = \tan^{-1}[(x - y)/(1 + xy)]$ , such that

$$\tan^{-1} \left( \frac{k_{30}}{\sqrt{k_1^2 + k_2^2}} \right) - \tan^{-1} \left( \frac{k_3}{\sqrt{k_1^2 + k_2^2}} \right) = \tan^{-1} \left( \frac{(k_{30} - k_3)\sqrt{k_1^2 + k_2^2}}{k_1^2 + k_2^2 + k_{30}k_3} \right).$$

Composing Equations (17–19) into matrix form,

$$\begin{bmatrix} dZ_1(\mathbf{k}; t) \\ dZ_2(\mathbf{k}; t) \\ dZ_3(\mathbf{k}; t) \end{bmatrix} = \begin{bmatrix} 1 & 0 & \zeta_1 \\ 0 & 1 & \zeta_1 \\ 0 & 0 & k_0^2/k^2 \end{bmatrix} \begin{bmatrix} dZ_1(\mathbf{k}_0; 0) \\ dZ_2(\mathbf{k}_0; 0) \\ dZ_3(\mathbf{k}_0; 0) \end{bmatrix}, \quad (20)$$

$$\zeta_1 = C_1 - \frac{k_2}{k_1} C_2, \quad (21)$$

$$\zeta_2 = \frac{k_2}{k_1} C_1 + C_2, \quad (22)$$

$$C_1 = \frac{k_1(k_{30}k^2 - k_3k_0^2)}{(k_1^2 + k_2^2)k^2}, \quad (23)$$

$$C_2 = \frac{k_2k_0^2}{(k_1^2 + k_2^2)^{3/2}} \tan^{-1} \left( \frac{(k_{30} - k_3)\sqrt{k_1^2 + k_2^2}}{k_1^2 + k_2^2 + k_{30}k_3} \right), \quad (24)$$

which is equivalent to Equations (3.14–3.17) of Mann (1994).

Assuming the postulate that the time-varying velocity spectral tensor can be made stationary by substituting an eddy-lifetime parameter  $\tau(k)$  in place of time  $t$ , the components of the tensor follow from Equation (2),

$$\begin{aligned} \frac{\langle dZ_i^*(\mathbf{k}; \tau) dZ_j(\mathbf{k}; \tau) \rangle}{d^3\mathbf{k}} &= \phi_{ij}(\mathbf{k}; \tau), \\ &= \phi_{ij}(\mathbf{k}). \end{aligned}$$

In like manner

$$\frac{\langle dZ_i^*(\mathbf{k}_0; 0) dZ_j(\mathbf{k}_0; 0) \rangle}{d^3\mathbf{k}} = \phi_{ij}(\mathbf{k}_0),$$

where  $\phi_{ij}(\mathbf{k}_0)$  is the spectral tensor for incompressible isotropic turbulent flow. The form of the initially isotropic spectral tensor is (Wyngaard 2010, p. 344),

$$\phi_{ij}(\mathbf{k}_0) = \frac{E(k_0)}{4\pi k_0^4} (\delta_{ij}k_0^2 - k_{0i}k_{0j}), \quad (25)$$

where  $E$  is the three-dimensional energy spectrum. By definition it is (Wyngaard 2010, p. 343)

$$E(k_0) = \iint_{k_0, k_{0i}=k_0^2} \frac{\phi_{ii}(\mathbf{k}_0)}{2} da, \quad (26)$$

which represents the contribution of all Fourier modes with turbulent wavenumber magnitude  $k_0$  to the turbulence kinetic energy. A form of the von Kármán energy spectrum is used by Mann (1994),

$$E(k) = \alpha \epsilon^{2/3} L^{5/3} \frac{(Lk)^4}{[1 + (Lk)^2]^{7/6}}, \quad (27)$$

where  $\alpha = 1.7$ ,  $\epsilon$  is the specific turbulent kinetic energy viscous dissipation rate, and  $L$  is a length scale. Components of the uniformly sheared velocity spectral tensor are (Mann 1994)

$$\begin{aligned} \phi_{11}(\mathbf{k}) &= \phi_{11}(\mathbf{k}_0) + \phi_{13}(\mathbf{k}_0)\zeta_1 + \phi_{31}(\mathbf{k}_0)\zeta_1 + \phi_{33}(\mathbf{k}_0)\zeta_1^2, \\ &= \frac{E(k_0)}{4\pi k_0^4} [k_0^2 - k_1^2 - 2k_1 k_{30}\zeta_1 + (k_1^2 + k_2^2)\zeta_1^2], \end{aligned} \quad (28)$$

$$\begin{aligned} \phi_{12}(\mathbf{k}) &= \phi_{11}(\mathbf{k}_0) + \phi_{13}(\mathbf{k}_0)\zeta_2 + \phi_{32}(\mathbf{k}_0)\zeta_1 + \phi_{33}(\mathbf{k}_0)\zeta_1\zeta_2, \\ &= \frac{E(k_0)}{4\pi k_0^4} [-k_1 k_2 - k_1 k_{30}\zeta_2 - k_2 k_{30}\zeta_1 + (k_1^2 + k_2^2)\zeta_1\zeta_2], \end{aligned} \quad (29)$$

$$\begin{aligned} \phi_{13}(\mathbf{k}) &= \phi_{13}(\mathbf{k}_0) \frac{k_0^2}{k^2} + \phi_{33}(\mathbf{k}_0)\zeta_1 \frac{k_0^2}{k^2}, \\ &= \frac{E(k_0)}{4\pi k_0^2 k^2} [-k_1 k_{30} + (k_1^2 + k_2^2)\zeta_1], \end{aligned} \quad (30)$$

$$\begin{aligned} \phi_{22}(\mathbf{k}) &= \phi_{22}(\mathbf{k}_0) + \phi_{23}(\mathbf{k}_0)\zeta_2 + \phi_{32}(\mathbf{k}_0)\zeta_2 + \phi_{33}(\mathbf{k}_0)\zeta_2^2, \\ &= \frac{E(k_0)}{4\pi k_0^4} [k_0^2 - k_2^2 - 2k_2 k_{30}\zeta_2 + (k_1^2 + k_2^2)\zeta_2^2], \end{aligned} \quad (31)$$

$$\begin{aligned} \phi_{23}(\mathbf{k}) &= \phi_{23}(\mathbf{k}_0) \frac{k_0^2}{k^2} + \phi_{33}(\mathbf{k}_0)\zeta_2 \frac{k_0^2}{k^2}, \\ &= \frac{E(k_0)}{4\pi k_0^2 k^2} [-k_2 k_{30} + (k_1^2 + k_2^2)\zeta_2], \end{aligned} \quad (32)$$

$$\begin{aligned} \phi_{33}(\mathbf{k}) &= \phi_{33}(\mathbf{k}_0) \frac{k_0^4}{k^4}, \\ &= \frac{E(k_0)}{4\pi k^4} (k_1^2 + k_2^2). \end{aligned} \quad (33)$$

#### 4.1 Effective eddy viscosity factor

By introducing an effective eddy viscosity an additional term is present in the evolution equation for stochastic increments. The  $dZ_3$  component in Equation (16) is

$$\frac{d}{dt} dZ_3(\mathbf{k}; t) = -\nu_t k^2 dZ_3(\mathbf{k}; t) + \frac{\partial U_1}{\partial x_3} \left( 2 \frac{k_1 k_3}{k_2} \right) dZ_3(\mathbf{k}; t).$$

As before, separation of variables leads to a solution. Integrating the additional term is straightforward:

$$\begin{aligned} -\nu_t \int_0^t k^2 dt' &= \frac{\nu_t}{k_1 (\partial U_1 / \partial x_3)} \int_{k_{30}}^{k_3} (k_1^2 + k_2^2 + k_3'^2) dk_3', \\ &= -\frac{\nu_t t}{k_3 - k_{30}} \left[ (k_1^2 + k_2^2)(k_3 - k_{30}) + (k_3^3 - k_{30}^3) / 3 \right], \\ &= -\nu_t t \left[ k_0^2 - k_1 k_{30} \beta + (k_1 \beta)^2 / 3 \right]. \end{aligned}$$

This is the argument in the exponential for  $D$  in Eq. (3.12.3) of (Townsend 1976, p. 83). Therefore, the solution for  $dZ_3$  is

$$dZ_3(\mathbf{k}; t) = e^{-\nu_t t [k_0^2 - k_1 k_{30} \beta + (k_1 \beta)^2 / 3]} \frac{k_0^2}{k^2} dZ_3(\mathbf{k}_0; 0).$$

As Savill (1987) notes, introducing an effective eddy viscosity to the rapid-distortion equation introduces an integrating factor, such that the original solution is simply corrected by dividing through by this factor. In particular, multiplying each term of Equation (20) by

$$D = e^{-\nu_t t [k_0^2 - k_1 k_{30} \beta + (k_1 \beta)^2 / 3]}$$

provides a solution to Equation (16).

## 4.2 Mass conservation

A physical check of Equation (20) is the satisfaction of mass conservation. In particular,  $k_i \phi_{ij}(\mathbf{k}) = 0$ . Expanding the  $j = 3$  component,

$$\begin{aligned}
k_i \phi_{i3}(\mathbf{k}) &= k_1 \phi_{13}(\mathbf{k}) + k_2 \phi_{23}(\mathbf{k}) + k_3 \phi_{33}(\mathbf{k}), \\
&= k_1 \frac{E(k_0)}{4\pi k_0^2 k^2} \left[ -k_1 k_{30} + (k_1^2 + k_2^2) \zeta_1 \right] + k_2 \frac{E(k_0)}{4\pi k_0^2 k^2} \left[ -k_2 k_{30} + (k_1^2 + k_2^2) \zeta_2 \right] \\
&\quad + k_3 \frac{E(k_0)}{4\pi k^4} (k_1^2 + k_2^2), \\
&= \frac{E(k_0)}{4\pi (k_0 k)^2} \left[ -k_{30} k_1^2 - k_{30} k_2^2 + (C_1 / k_1) (k_1^2 + k_2^2)^2 + k_3 (k_1 k_0 / k)^2 + k_3 (k_2 k_0 / k)^2 \right], \\
&= 0.
\end{aligned}$$

This can be shown to be true for  $j = 1$  and  $2$ , as well. Equation (20) satisfies mass conservation.

## 5 Eddy-Lifetime Parameter

A scale-varying eddy-lifetime parameter is proposed by Mann (1994) as a timescale during which an eddy is formed and breaks up. This parameter, as noted in Section 4, is central to the postulate that the time-varying velocity spectral tensor can be made stationary. The form proposed is

$$\tau(k) \propto k^{-1} \left[ \int_k^\infty E(k') dk' \right]^{-1/2}, \quad (34)$$

where the eddy lifetime is considered proportional to its size  $k^{-1}$  divided by its characteristic velocity, approximated as  $\left( \int_k^\infty E(k') dk' \right)^{1/2}$ . This definition is used to extend the notion of an eddy-lifetime to eddies in the energy subrange of turbulence. Substituting Equation (27) into the integral of the energy spectrum and making the variable substitution  $s = (k/k')^2$  and  $dk' = (-1/2)s^{-3/2}k ds$  gives

$$\begin{aligned} \int_k^\infty E(k') dk' &= \int_k^\infty \alpha \epsilon^{2/3} L^{5/3} \frac{(Lk')^4}{[1 + (Lk')^2]^{17/6}} dk', \\ &= \frac{\alpha}{2} \epsilon^{2/3} k^{-2/3} \int_0^1 \frac{s^{-2/3}}{[1 + (kL)^{-2}s]^{17/6}} ds, \\ &= \frac{\alpha}{2} \epsilon^{2/3} k^{-2/3} \frac{\Gamma(1/3)}{\Gamma(4/3)} {}_2F_1(17/6, 1/3; 4/3; -(kL)^{-2}), \end{aligned}$$

where the hypergeometric function has the following integral form (DLMF, Eq. 15.6.1),

$${}_2F_1(a, b; c; z) = \frac{\Gamma(c)}{\Gamma(b)\Gamma(c-b)} \int_0^1 \frac{t^{b-1}(1-t)^{c-b-1}}{(1-zt)^a} dt.$$

It is unclear why the first and second arguments of the hypergeometric function are switched in Equation (3.3) of Mann (1994). However, switching these arguments leaves the value of the hypergeometric function unchanged as can be seen by its infinite series definition (DLMF, Equation 15.2.1):

$${}_2F_1(a, b; c; z) = \frac{\Gamma(c)}{\Gamma(a)\Gamma(b)} \sum_{s=0}^{\infty} \frac{\Gamma(a+s)\Gamma(b+s)}{\Gamma(c+s)s!} z^s.$$

An alternative solution for the integral expression is based on a rather straightforward substitution  $q = 1 - s$ ,  $dq = -ds$  :

$$\begin{aligned} \int_k^{\infty} E(k') dk' &= \frac{\alpha}{2} \epsilon^{2/3} k^{-2/3} \int_0^1 \frac{s^{-2/3}}{[1 + (kL)^{-2}s]^{17/6}} ds, \\ &= \frac{\alpha}{2} (\epsilon L)^{2/3} (kL)^{-2/3} \frac{(kL)^{17/3}}{[1 + (kL)^2]^{17/6}} \int_0^1 \frac{(1-q)^{-2/3}}{[1 - [1 + (kL)^2]^{-1}q]^{17/6}} dq, \quad (35) \\ &= \frac{\alpha}{2} (\epsilon L)^{2/3} \frac{(kL)^5}{[1 + (kL)^2]^{17/6}} \frac{\Gamma(1/3)}{\Gamma(4/3)} {}_2F_1(17/6, 1; 4/3; [1 + (kL)^2]^{-1}). \end{aligned}$$

This representation is particularly important for numerically evaluating the vertical velocity variance  $\langle u_3 u_3 \rangle$  since the  $z = [1 + (kL)^2]^{-1}$  argument of the hypergeometric function satisfies the condition  $|z| < 1$  for  $k \in (0, \infty)$ . In contrast, the alternate form by Mann (1994),  $z = -(kL)^{-2}$ , does not satisfy the condition  $|z| < 1$  for all  $k$ . When  $k < 1/L$ , then  $|z| > 1$ . In this case some transformation formula must be applied to map  $z$  to some region within the complex-valued unit disc in order to compute the hypergeometric function. It should be further noted that Equation (35) still maintains the same limiting characteristics in the eddy-lifetime parameter, as  $k$  goes to zero ( $\tau \propto k^{-1}$ ) or infinity ( $\tau \propto k^{-2/3}$ ).

Instead of Equation (27), the following energy spectrum function is used throughout the remainder of this tutorial (Wilson 2000):

$$E(k) = \frac{55}{9B(1/2, 1/3)} \frac{\sigma^2 k^4 \ell^5}{[1 + (k\ell)^2]^{17/6}}, \quad (36)$$

where  $\sigma^2$  is the isotropic velocity variance,  $\ell$  is a length scale, and  $B(x, y) = \Gamma(x)\Gamma(y) / \Gamma(x+y)$ . This form for the energy spectrum function is equivalent to Equation (27), provided  $\ell = L$ , and  $\sigma^2 = 9B(1/2, 1/3)\alpha(\epsilon L)^{2/3} / 55$ . Integrating Equation (36) over all wavenumber magnitudes gives the turbulence kinetic energy for isotropic turbulence, that is,

$$\frac{\langle u_i u_i \rangle}{2} = \frac{3\sigma^2}{2} = \int_0^\infty E(k) dk,$$

where  $\langle u_i u_i \rangle$  is evaluated at time zero. The integral for squared characteristic eddy velocity, following the same substitutions as above, is

$$\int_k^\infty E(p) dp = \frac{55}{18B(1/2, 1/3)} \frac{\sigma^2 (k\ell)^5}{[1 + (k\ell)^2]^{7/6}} \frac{\Gamma(1/3)}{\Gamma(4/3)} {}_2F_1(17/6, 1; 4/3; [1 + (k\ell)^2]^{-1}). \quad (37)$$

By Equation (34), the eddy lifetime is proportional in the following manner:

$$\tau(k) \propto \sqrt{\frac{6B(1/2, 1/3)}{55}} \left( \frac{\ell}{\sigma} \right) \frac{[1 + (k\ell)^2]^{17/12}}{(k\ell)^{7/2}} \left[ {}_2F_1(17/6, 1; 4/3; [1 + (k\ell)^2]^{-1}) \right]^{-1/2}.$$

Introducing the proportionality factor  $\sqrt{55/6B(1/2, 1/3)} \Upsilon (\partial U_1 / \partial x_3)^{-1} (\sigma / \ell)$  gives an alternative to Equation (3.6) of Mann (1994):

$$\tau(k) = \Upsilon \left( \frac{\partial U_1}{\partial x_3} \right)^{-1} \frac{[1 + (k\ell)^2]^{17/12}}{(k\ell)^{7/2}} \left[ {}_2F_1(17/6, 1; 4/3; [1 + (k\ell)^2]^{-1}) \right]^{-1/2}, \quad (38)$$

where  $\Upsilon$  is a dimensionless shear anisotropy parameter.

## 6 Turbulence Kinetic Energy Budget

The turbulence kinetic energy (TKE) budget is an evolution equation for the mean kinetic energy per unit mass of the turbulence (Wyngaard 2010, Equation (5.42)):

$$\frac{1}{2} \frac{\partial}{\partial t} \langle u_i u_i \rangle = -\frac{U_j}{2} \frac{\partial}{\partial x_j} \langle u_i u_i \rangle - \langle u_i u_j \rangle \frac{\partial U_i}{\partial x_j} - \frac{1}{2} \frac{\partial}{\partial x_j} \langle u_i u_i u_j \rangle - \frac{1}{\rho} \frac{\partial}{\partial x_i} \langle p u_i \rangle - \nu \left\langle \frac{\partial u_i}{\partial x_j} \frac{\partial u_i}{\partial x_j} \right\rangle, \quad (39)$$

where the right-hand side terms represent mean advection, mean-gradient production, turbulent transport, pressure-gradient interaction, and viscous dissipation, respectively. A corresponding TKE budget equation arises through manipulation of the uniform shear rapid distortion equation. Premultiplying Equation (15) with  $dZ_i^*$ , taking the complex conjugate of Equation (15) and premultiplying by  $dZ_i$ , summing these two equations, and ensemble averaging gives

$$\begin{aligned} \frac{d}{dt} \langle dZ_i^*(\mathbf{k}; t) dZ_i(\mathbf{k}; t) \rangle &= -\frac{\partial U_1}{\partial x_3} \langle dZ_1(\mathbf{k}; t) dZ_3^*(\mathbf{k}; t) + dZ_1^*(\mathbf{k}; t) dZ_3(\mathbf{k}; t) \rangle, \\ \frac{d}{dt} \phi_{ii}(\mathbf{k}; t) d^3 \mathbf{k} &= -\frac{\partial U_1}{\partial x_3} [\phi_{13}^*(\mathbf{k}; t) + \phi_{13}(\mathbf{k}; t)] d^3 \mathbf{k}, \end{aligned}$$

where the condition for mass conservation,  $k_i dZ_i = 0$ , is applied.

Integrating the above expression over all turbulence wavenumbers yields

$$\begin{aligned} \frac{d}{dt} \iiint_{-\infty}^{\infty} \phi_{ii}(\mathbf{k}; t) d^3 \mathbf{k} &= -\frac{\partial U_1}{\partial x_3} \iiint_{-\infty}^{\infty} [\phi_{31}(\mathbf{k}; t) + \phi_{13}(\mathbf{k}; t)] d^3 \mathbf{k}, \\ \frac{d}{dt} \langle u_i u_i \rangle &= -\frac{\partial U_1}{\partial x_3} [\langle u_3 u_1 \rangle + \langle u_1 u_3 \rangle], \\ &= -2 \frac{\partial U_1}{\partial x_3} \langle u_1 u_3 \rangle, \end{aligned}$$

where commutativity is assumed for the total time derivative and integration over turbulent wavenumbers. Rearranging terms gives

$$\frac{1}{2} \frac{\partial}{\partial t} \langle u_i u_i \rangle = -\frac{U_j}{2} \frac{\partial}{\partial x_j} \langle u_i u_i \rangle - \langle u_1 u_3 \rangle \frac{\partial U_1}{\partial x_3}. \quad (40)$$

In comparison to Equation (39), the TKE budget for rapid distortion theory contains mean advection and one term for mean-gradient transport due to uniform shear. Furthermore, it neglects turbulent transport, pressure-gradient interaction, and viscous dissipation. Under some circumstances some of these assumptions may be justifiable. For example, in a horizontally homogeneous, quasi-steady boundary layer flow, absent buoyancy effects, the TKE balance near the surface is (Wyngaard 2010, p. 105)

$$\frac{1}{2} \frac{\partial}{\partial t} \langle u_i u_i \rangle = 0 = -\langle u_1 u_3 \rangle \frac{\partial U_1}{\partial x_3} - \epsilon.$$

However, it should be noted that pressure-gradient interaction terms are responsible for intercomponent TKE transfer (Wyngaard 2010, p. 105). Therefore, the simplifications inherent to Equation (12) necessarily limit its general applicability.

Despite the assumptions inherent in Equation (40) a nondimensional form serves as a useful check for computational purposes. Making the substitution  $\beta = (\partial U_1 / \partial x_3) t$  for the total time derivative, dividing both sides by isotropic velocity variance  $\sigma^2$ , and integrating from zero to  $\beta$  gives

$$\begin{aligned} \int_0^\beta d \left( \frac{\langle u_i u_i \rangle}{\sigma^2} \right) &= -2 \int_0^\beta \frac{\langle u_1 u_3 \rangle}{\sigma^2} d\beta', \\ \frac{\langle u_i u_i \rangle}{\sigma^2} - 3 &= -2 \int_0^\beta \frac{\langle u_1 u_3 \rangle}{\sigma^2} d\beta'. \end{aligned} \tag{41}$$

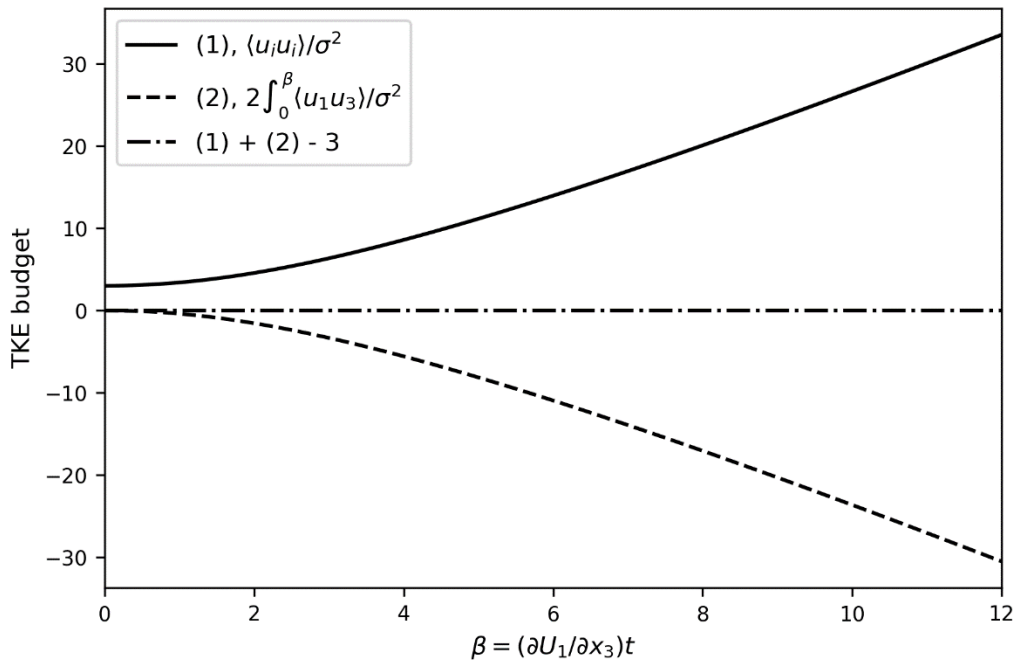
Furthermore, this expression is a useful check against approximations for velocity covariances after small times ( $\beta < 1$ ). For example, per Equation (41), Equation (3.12.5) of Townsend (1976),

$$\begin{aligned}
\frac{\langle u_1 u_1 \rangle}{\sigma^2} &= 1 + \frac{2}{7} \beta^2, \\
\frac{\langle u_2 u_2 \rangle}{\sigma^2} &= 1 + \frac{8}{35} \beta^2, \\
\frac{\langle u_3 u_3 \rangle}{\sigma^2} &= 1 - \frac{4}{35} \beta^2, \\
\frac{\langle u_1 u_3 \rangle}{\sigma^2} &= -\frac{2}{5} \beta,
\end{aligned} \tag{42}$$

satisfies the balance in the TKE budget for  $\beta < 1$ . For  $\beta > 1$  this approximation is no longer valid.

Figure 1 gives an illustration of the integrated material derivative of TKE, and the integrated mean-gradient production, as in Equation (41). The mean-gradient production of TKE continuously feeds the combined time rate of change and mean-advection of TKE. Without viscous dissipation, TKE grows without bound, a nonphysical aspect of RDT.

Figure 1. Rapid distortion theory integrated TKE budget terms as a function of nondimensional time  $\beta$ .



## 7 Shear-Distorted Velocity Covariances, Spectra, and Length Scales

Before introducing predictions of shear-distorted velocity covariances, one-dimensional spectra, and length scales, it is worth noting that all results are presented in a nondimensional form. In particular, a turbulent wavenumber is made dimensionless by taking the product with length scale  $\ell$ , that is  $n_i = k_i \ell$ . As a consequence the energy spectrum function of Equation (36) is made dimensionless by dividing by the product of isotropic velocity variance and length scale

$$\frac{E(n)}{\sigma^2 \ell} = \frac{55}{9B(1/2, 1/3)} \frac{n^4}{(1+n^2)^{17/6}}, \quad (43)$$

where  $n^2 = n_1^2 + n_2^2 + n_3^2$ . The velocity spectral tensor is made dimensionless by dividing by the product of isotropic velocity variance and length scale cubed, that is,  $\phi_{ij}(\mathbf{n}) / \sigma^2 \ell^3$ , where  $\mathbf{n} = (n_1, n_2, n_3)$ . As such, the velocity covariances obtained by integrating the normalized velocity spectral tensor are a normalized covariance

$$\frac{\langle u_i u_j \rangle}{\sigma^2} = \iiint_{-\infty}^{\infty} \frac{\phi_{ij}(\mathbf{n})}{\sigma^2 \ell^3} d^3 \mathbf{n}. \quad (44)$$

Streamwise one-dimensional spectra are normalized similarly to the energy spectrum function,

$$\frac{F_{ij}^1(n_1)}{\sigma^2 \ell} = \iint_{-\infty}^{\infty} \frac{\phi_{ij}(\mathbf{n})}{\sigma^2 \ell^3} dn_2 dn_3. \quad (45)$$

For a turbulent streamwise wavenumber  $\hat{n}_1$ , such that

$$\left. \frac{d}{dn_1} \left( n_1 \frac{F_{ij}^1(n_1)}{\sigma^2 \ell} \right) \right|_{n_1=\hat{n}_1} = 0,$$

normalized length scales are

$$\frac{\ell_{ij}}{\ell} = \frac{1}{\hat{n}_1}, \quad (46)$$

where  $\ell_{ij}$  are length scales for the streamwise one-dimensional spectra  $F_{ij}^1(n_1)$ .

Equations (44) and (45) were numerically evaluated using Cubature, a package for adaptive multidimensional integration by Johnson (2017). A wrapper for this package was used for evaluation in Python 3 (Castro et al. 2018). The Cubature package provides a vectorized interface, which was used to evaluate the nondimensional velocity spectral tensor on a logarithmically spaced vector of 200 streamwise wavenumbers for Equation (45) in a matter of minutes on a personal workstation.

Velocity (co)variances for the nonstationary spectral tensor are shown in Figure 2. As required by isotropy, for  $\beta = 0$  all normalized velocity variances are equivalent and equal to one. The increases in streamwise velocity variance and negative velocity covariance  $-\langle u_1 u_3 \rangle$  is attributed to horizontal momentum changes due to vertical motion caused by shear (Hunt and Carruthers 1990). An important distinction in this comparison is that velocity (co)variances shown here evolve over time. On the other hand, Figure 4(a) in Mann (1994) illustrates velocity (co)variances under varying stationary conditions. In this sense the similarities between the two figures obscure very important differences.

For nondimensional time  $\beta = 1$ , normalized premultiplied one-dimensional spectra are shown in Figure 3. For this particular time the peak of the transverse velocity spectrum  $n_1 F_{22}^1$  exceeds the streamwise component  $n_1 F_{11}^1$ , which is not typical of atmospherically stable near-surface turbulence (Chougule et al. 2018). However, the situation is less clear under atmospherically unstable conditions, cf. Figures 4 and 5 of Chougule et al. (2018). Another point of comparison is the lower turbulent wavenumber peak in the vertical velocity spectrum  $n_1 F_{33}^1$  relative to the transverse velocity spectrum. Under both atmospherically unstable and stable conditions, experimental evidence shows an opposite relationship (Chougule et al. 2018). For this particular  $\beta$  the predicted relationship is not physical.

Figure 2. Normalized velocity (co)variances as a function of nondimensional time  $\beta$ .

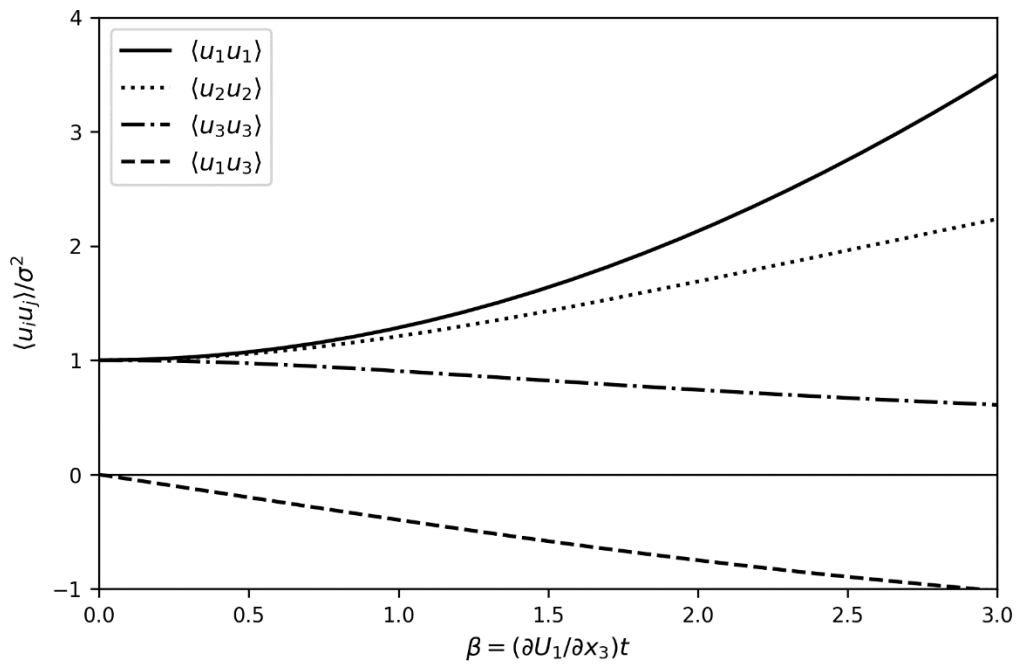


Figure 3. Normalized premultiplied one-dimensional spectra as a function of nondimensional streamwise wavenumber  $n_1$ . Nondimensional time  $\beta = 1$ .

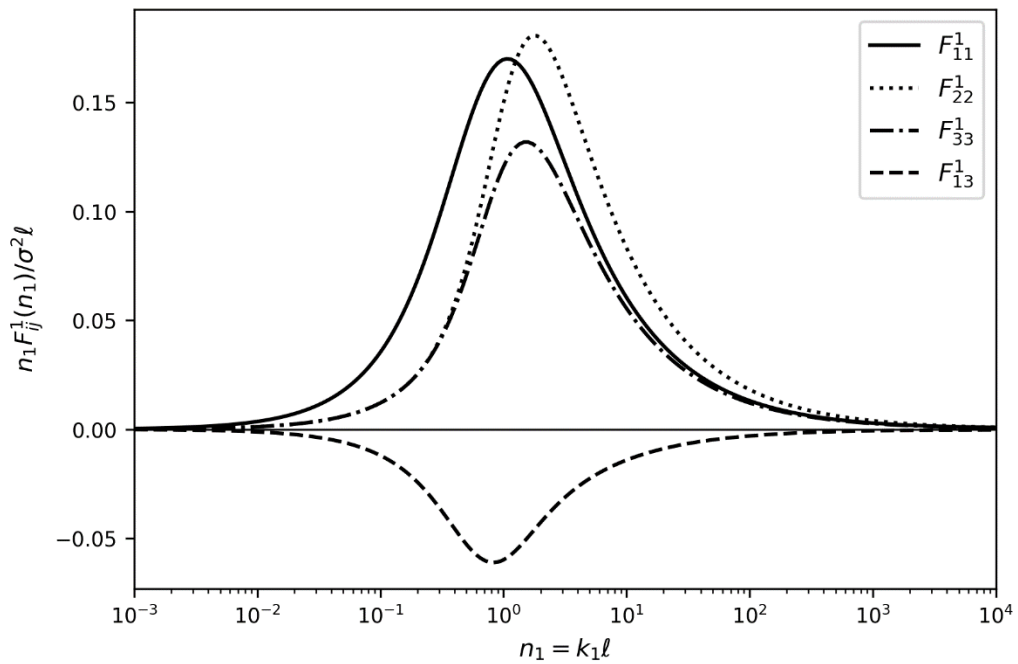


Figure 4 is a version of Figure 3 on log-log axes. This representation shows the power-law features of streamwise one-dimensional spectra. Beyond the peak in the figure, the premultiplied spectra fall off as  $n_1^{-2/3}$ , which goes as  $n_1^{-5/3}$  for the spectra. This power-law feature is termed Kolmogorov scaling and is indicative of an inertial subrange. Within this range, turbulence contains length scales between the largest and smallest scales. The rate of gain in TKE from the largest scales of turbulence is balanced by the rate of TKE loss by the smallest scales of turbulence, otherwise known as an energy cascade (Wyngaard 2010, pp. 145–147).

**Figure 4.** Normalized premultiplied one-dimensional spectra as a function of nondimensional streamwise wavenumber  $n_1$ . Nondimensional time  $\beta = 1$ . Both axes are logarithmically scaled.

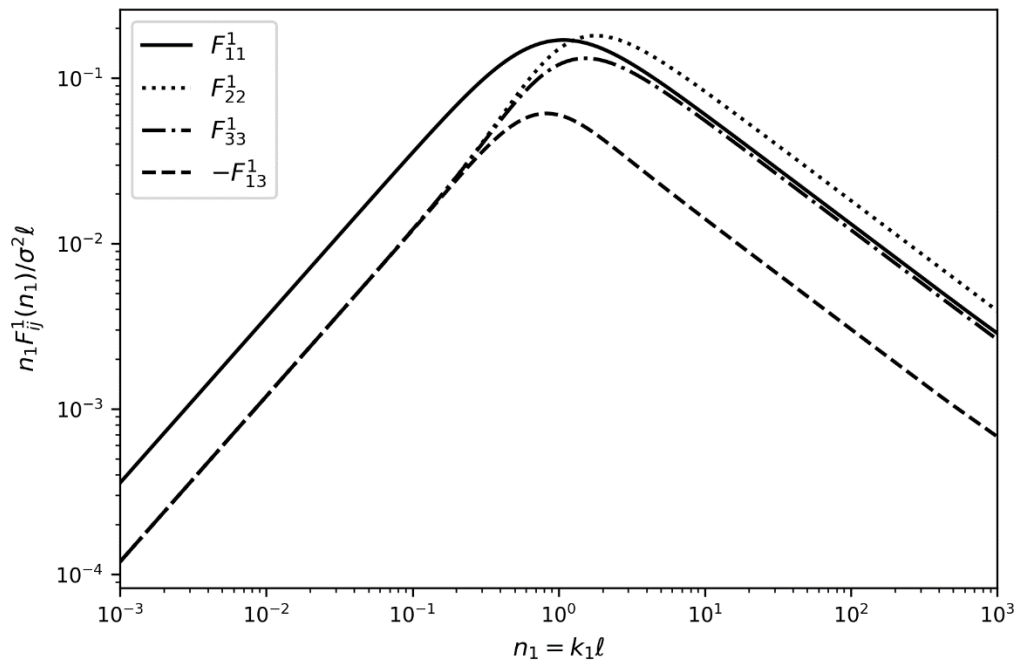
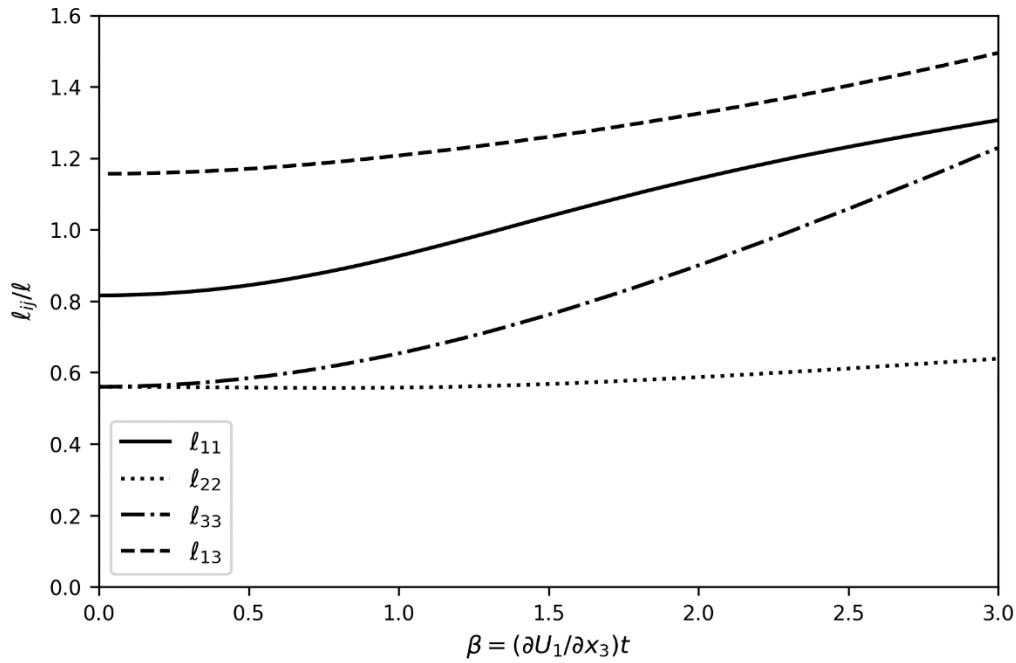


Figure 5 illustrates the evolution of normalized length scales as a function of nondimensional time  $\beta$ .

Figure 5. Normalized length scales as a function of nondimensional time  $\beta$ .

Under isotropic conditions the normalized length scales are (Mann 1994)

$$\frac{\ell_{11}}{\ell} = \sqrt{2/3},$$

$$\frac{\ell_{22}}{\ell} = \frac{\ell_{33}}{\ell} = 2(6 + 3\sqrt{5})^{-1/2},$$

which can be derived from Equation (46) and the analytical expressions for the one-dimensional velocity spectra,

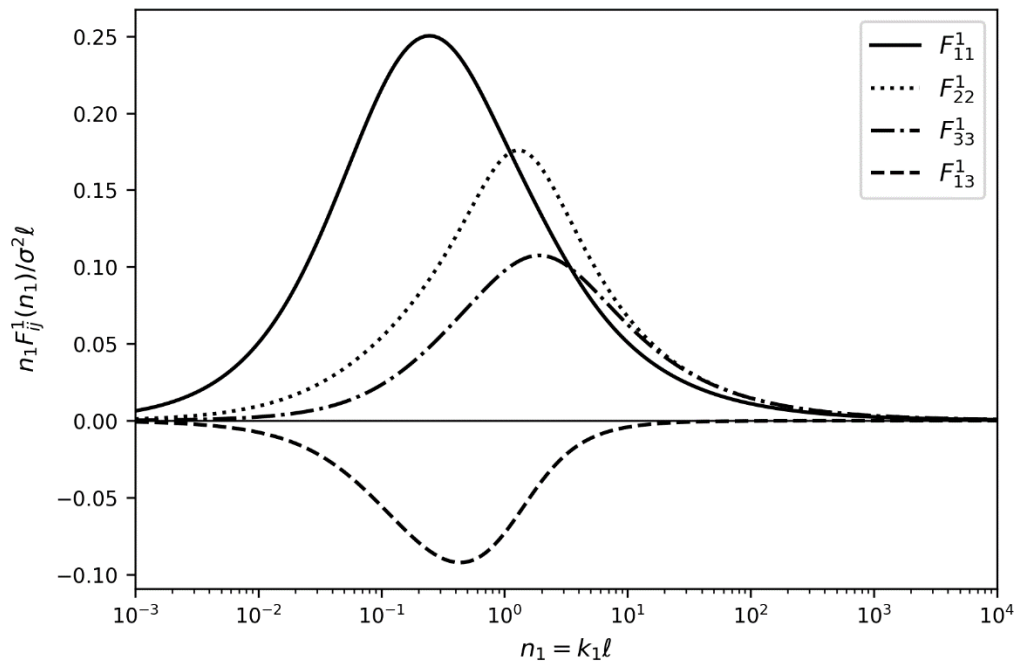
$$\frac{F_{11}^1(n_1)}{\sigma^2 \ell} = \frac{1}{B(1/2, 1/3)} \frac{1}{(1 + n_1^2)^{5/6}},$$

$$\frac{F_{22}^1(n_1)}{\sigma^2 \ell} = \frac{F_{33}^1(n_1)}{\sigma^2 \ell} = \frac{1}{6B(1/2, 1/3)} \frac{3 + 8n_1^2}{(1 + n_1^2)^{11/6}}.$$

It is evident that for all times greater than zero  $\ell_{33}$  exceeds  $\ell_{22}$  and apparently at some point for  $\beta > 3$  will exceed  $\ell_{11}$ . This shows how RDT, in its unmodified form, is unsuitable for near-surface atmospheric turbulence.

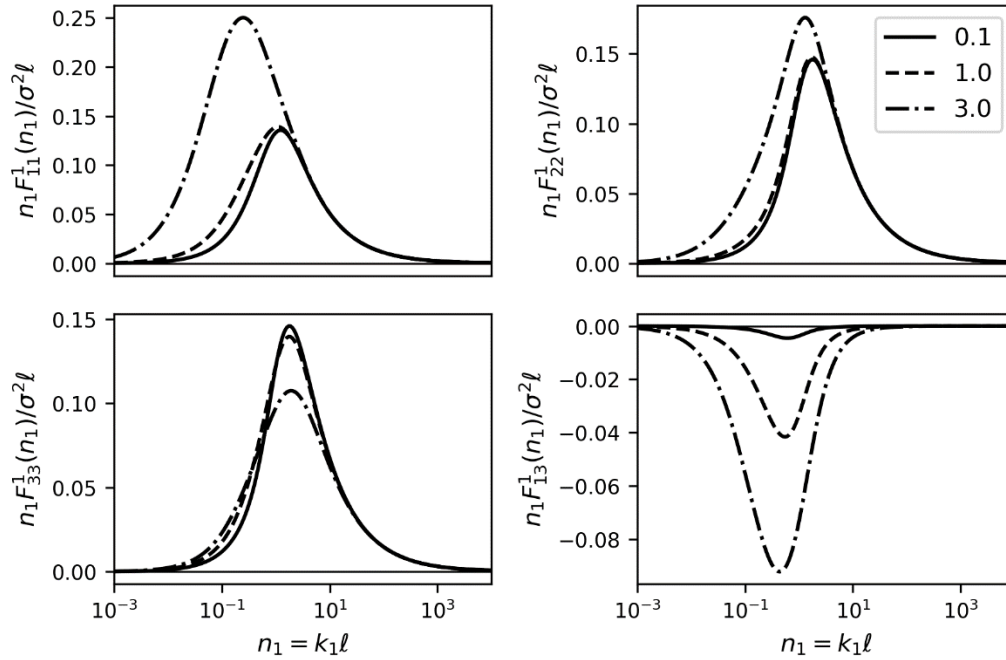
Figure 6 shows *stationary* premultiplied one-dimensional spectra for shear anisotropy parameter  $\Upsilon = 3$ . In contrast to Figure 3, the peak of  $n_1 F_{22}^1$  is less than  $n_1 F_{11}^1$ , and its peak is lower in streamwise wavenumber than  $n_1 F_{33}^1$ . This translates into  $\ell_{22}$  being greater than  $\ell_{33}$ , which is typical for experimental measurements of near-surface turbulence. Another distinguishing characteristic is the low wavenumber skew in the cospectrum  $n_1 F_{13}^1$ , as opposed to the high wavenumber skew in Figure 3, an indicator that relatively more energy resides below the premultiplied spectral mode.

Figure 6. Normalized premultiplied one-dimensional spectra as a function of nondimensional streamwise wavenumber  $n_1$ . Shear anisotropy parameter  $\Upsilon = 3$ .



Stationary premultiplied one-dimensional spectra are shown for various shear anisotropy  $\Upsilon$  values in Figure 7. Relatively large increases in peak amplitude and length scale is evident for  $n_1 F_{11}^1$ . Relatively modest increases in peak amplitude and length scale for  $n_1 F_{22}^1$  arise as shear anisotropy increases, while the opposite is true for  $n_1 F_{33}^1$ . The length scales derived from premultiplied spectra are illustrated in Figure 4(b) of Mann (1994). As noted, the length scales take the order of  $\ell_{11} > \ell_{22} > \ell_{33}$ , which is experimentally observed.

Figure 7. Normalized premultiplied one-dimensional spectra as a function of nondimensional streamwise wavenumber  $n_1$ . Shear anisotropy parameter  $\Upsilon$  varies according to the legend.



## Second Invariant for the Velocity Anisotropy Tensor

One way to characterize the distortion of different flows is through the second invariant  $\Pi_u$  for the velocity anisotropy tensor (Hunt and Carruthers 1990),

$$\Pi_u = -\frac{1}{2} b_{ij} b_{ji}, \quad (47)$$

$$b_{ij} = \frac{\langle u_i u_j \rangle}{\langle u_i u_i \rangle} - \frac{1}{3} \delta_{ij}, \quad (48)$$

where the moments of velocity  $b_{ij}$ , and their product is

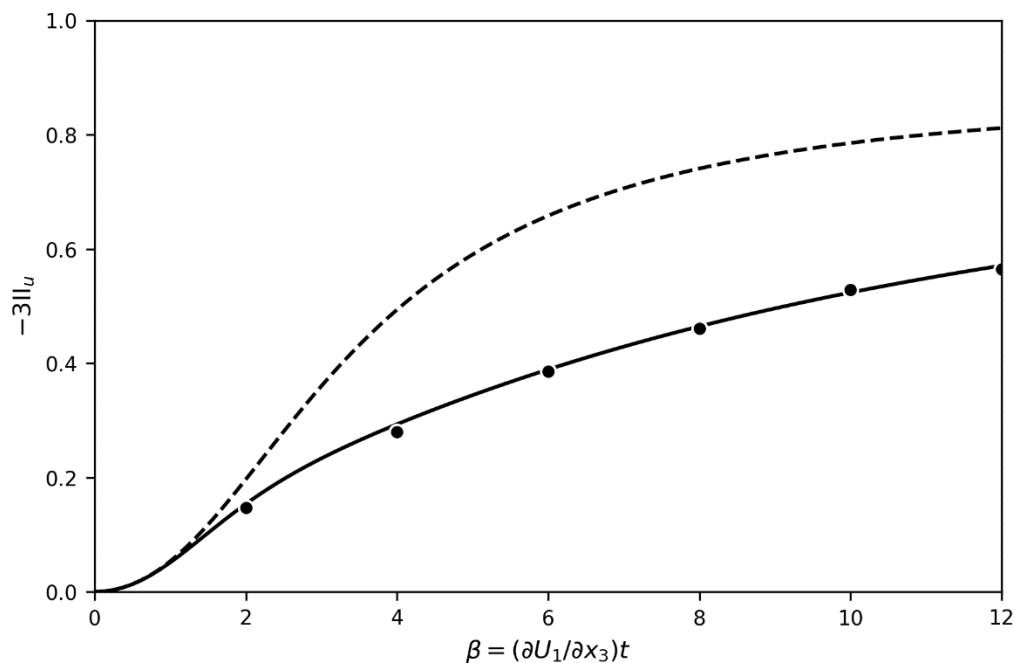
$b_{ij} b_{ji} = b_{11}^2 + b_{22}^2 + b_{33}^2 + 2b_{12}^2 + 2b_{13}^2 + 2b_{23}^2$ . The terms  $b_{12}$  and  $b_{23}$  are zero since the only nonzero shear term is  $\partial U_1 / \partial x_3$ . Equation (47) describes the anisotropy levels of large-scale turbulence.

In the limit of infinite strain ( $\beta \rightarrow \infty$ )  $-\Pi_u = 0.33$ , and the second invariant for the vorticity anisotropy tensor  $-\Pi_v = 0.083$  (Hunt and Carruthers 1990). As a consequence, the structure of turbulence becomes one-

dimensional in velocity such that streamwise velocity fluctuations are very large compared to transverse or vertical fluctuations. Furthermore, the turbulence becomes two-dimensional in vorticity such that transverse and vertical fluctuations in vorticity are much larger compared to streamwise fluctuations.

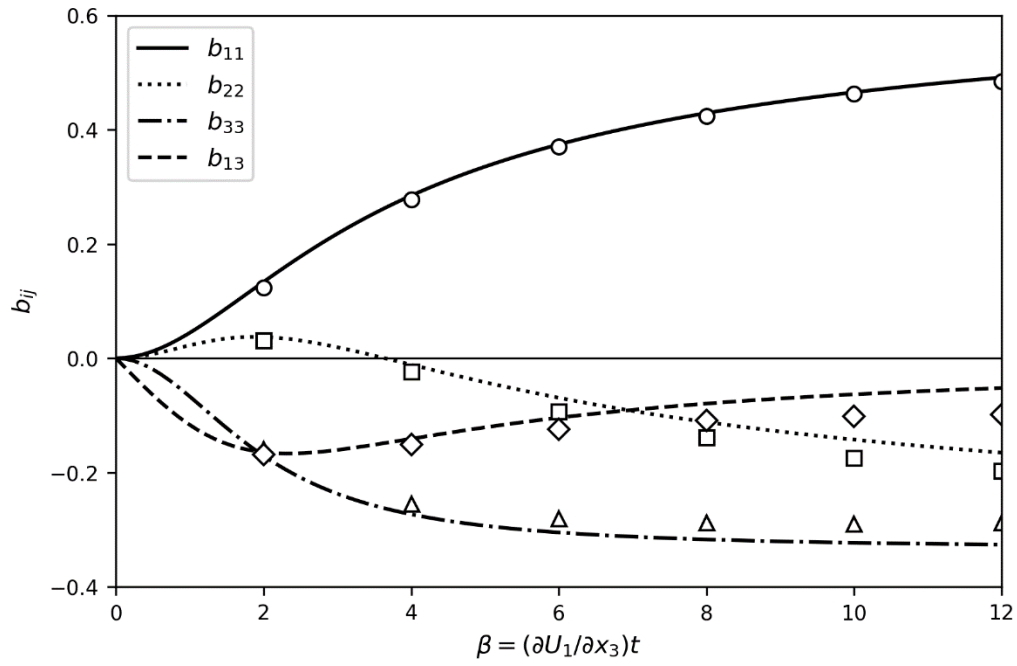
Figure 8 shows RDT predictions alongside direct numerical simulations of the viscous Navier-Stokes equations (Lee et al. 1990), and an early time approximation of Equation (42). The numerical solution by RDT, contrary to discussion by Hunt and Carruthers (1990), does not underestimate the anisotropy. In contrast to computations by Lee et al. (1990), the early time solution ( $\beta < 1$ ) is matched well by the approximation of Townsend (1976), Equation (42). This suggests that for high strain rate conditions the RDT prediction for anisotropy is fairly adequate for large-scale motions.

**Figure 8.** Second invariant for the velocity anisotropy tensor as a function of nondimensional time  $\beta$ ; solid line: from Equation (44), dashed line: from Equation (42), filled circles: DNS results from Lee et al. (1990).



The main reason there is better agreement between DNS simulations and predictions by RDT in Figure 8 is due to improved predictions of velocity moment  $b_{11}$ , as seen in Figure 9. Errors in all other velocity moments are the same as reported by Lee et al. (1990); however, the RDT prediction for  $b_{11}$  is different due to the corrected expression for  $\phi_{11}(\mathbf{k})$  by Mann (1994).

Figure 9. Moments of velocity  $b_{ij}$  as a function of nondimensional time  $\beta$ ; symbols: DNS results from Lee et al. (1990).



## 8 Conclusion

The derivation of the rapid-distortion theory equation is reproduced here, along with the analytical solution to the uniform shear rapid distortion equation, Equations (20–24), which was reported earlier by Mann (1994). It is shown how this solution satisfies both mass conservation and balance in the turbulence kinetic energy budget of Equation (40). An alternative expression for the eddy-lifetime parameter of Mann (1994, Equation 3.3) is given by Equation (38). This expression is crucial to computing the vertical velocity variance by numerical integration. Lastly, predictions of the second invariant for the velocity anisotropy tensor are shown to agree better with DNS than previously reported by Lee et al. (1990).

The findings here support closer examination of recent velocity spectral tensor models that include both uniform shear and temperature stratification (Chougule et al. 2017, 2018). Future work will consider how these turbulence models can be incorporated into the theory of near-surface atmospheric wind noise.

## References

- Batchelor, G. K. 1953. *The Theory of Homogeneous Turbulence*. Cambridge, UK: Cambridge University Press.
- Cambon, C., and J. F. Scott. 1999. "Linear and Nonlinear Models of Anisotropic Turbulence." *Annual Review of Fluid Mechanics* 31 (1): 1–53. doi:10.1146/annurev.fluid.31.1.1.
- Castro, S. G. P., A. Loukianov, scku208, M. Dewing, J. Bernardo Oliveira, D. Arnold, and A. Eljarrat. 2018. "Python Wrapper for Cubature: Adaptive Multidimensional Integration. Accessed August 2020. <https://zenodo.org/record/3715624/#.YG4yuK9KiUl>. Version 0.14.5.
- Chougule, A., J. Mann, M. Kelly, and G. C. Larsen. 2017. "Modeling Atmospheric Turbulence via Rapid Distortion Theory: Spectral Tensor of Velocity and Buoyancy." *Journal of the Atmospheric Sciences* 74 (4): 949–74. doi:10.1175/JAS-D-16-0215.1.
- Chougule, A., J. Mann, M. Kelly, and G. C. Larsen. 2018. "Simplification and Validation of a Spectral-Tensor Model for Turbulence including Atmospheric Stability." *Boundary-Layer Meteorology* 167 (3): 371–97. doi:10.1007/s10546-018-0332-z.
- DLMF. 2020. *NIST Digital Library of Mathematical Functions*. <http://dlmf.nist.gov/>. Release 1.0.27 of 2020-06-15. Edited by F. W. J. Olver, A. B. Olde Daalhuis, D. W. Lozier, B. I. Schneider, R. F. Boisvert, C. W. Clark, B. R. Miller, B. V. Saunders, H. S. Cohl, and M. A. McClain.
- Glegg, S., and W. Devenport. 2017. *Aeroacoustics of Low Mach Number Flows*. Oxford, UK: Academic Press.
- Hunt, J. C. R., and D. J. Carruthers. 1990. "Rapid Distortion Theory and the 'Problems' of Turbulence." *Journal of Fluid Mechanics* 212: 497–532. doi:10.1017/S0022112090002075.
- Johnson, S. G. "Cubature Package." Version 1.0.3. Accessed August 2020. <https://github.com/stevengi/cubature>.
- Kraichnan, R. H. 1956. "Pressure Fluctuations in Turbulent Flow over a Flat Plate." *The Journal of the Acoustical Society of America* 28 (3): 378–90. doi:10.1121/1.1908336.
- Lee, M. J., J. Kim, and P. Moin. 1990. "Structure of Turbulence at High Shear Rate." *Journal of Fluid Mechanics* 216: 561–583. doi:10.1017/S0022112090000532.
- Mann, J. 1994. "The Spatial Structure of Neutral Atmospheric Surface-Layer Turbulence." *Journal of Fluid Mechanics* 273: 141–68. doi:10.1017/S0022112094001886.
- Raspet, R., J. Yu, and J. Webster. 2008. "Low Frequency Wind Noise Contributions in Measurement Microphones." *The Journal of the Acoustical Society of America* 123 (3):1260–69. doi:10.1121/1.2832329.

- Savill, A. M. 1987. "Recent Developments in Rapid-Distortion Theory." *Annual Review of Fluid Mechanics* 19 (1): 531–73. doi:10.1146/annurev.fl.19.010187.002531.
- Townsend, A. A. 1970. "Entrainment and the Structure of Turbulent Flow." *Journal of Fluid Mechanics* 41 (1): 13–46. doi:10.1017/S0022112070000514.
- Townsend, A. A. 1976. *The Structure of Turbulent Shear Flow*. 2nd ed. Cambridge, UK: Cambridge University Press.
- Wilson, D. K. 2000. "A Turbulence Spectral Model for Sound Propagation in the Atmosphere that Incorporates Shear and Buoyancy Forcings." *The Journal of the Acoustical Society of America* 108 (5): 2021–38. doi:10.1121/1.1311779.
- Wyngaard, J. C. 2010. *Turbulence in the Atmosphere*. Cambridge, UK: Cambridge University Press. doi:10.1017/CBO9780511840524.
- Yu, J., R. Raspet, J. Webster, and J. Abbott. 2011. "Improved Prediction of the Turbulence-Shear Contribution to Wind Noise Pressure Spectra." *The Journal of the Acoustical Society of America* 130 (6): 3590–94. doi:10.1121/1.3652868.

# REPORT DOCUMENTATION PAGE

Form Approved  
OMB No. 0704-0188

Public reporting burden for this collection of information is estimated to average 1 hour per response, including the time for reviewing instructions, searching existing data sources, gathering and maintaining the data needed, and completing and reviewing this collection of information. Send comments regarding this burden estimate or any other aspect of this collection of information, including suggestions for reducing this burden to Department of Defense, Washington Headquarters Services, Directorate for Information Operations and Reports (0704-0188), 1215 Jefferson Davis Highway, Suite 1204, Arlington, VA 22202-4302. Respondents should be aware that notwithstanding any other provision of law, no person shall be subject to any penalty for failing to comply with a collection of information if it does not display a currently valid OMB control number. PLEASE DO NOT RETURN YOUR FORM TO THE ABOVE ADDRESS.

<b>1. REPORT DATE (DD-MM-YYYY)</b> 07/2022			<b>2. REPORT TYPE</b> Final Report		<b>3. DATES COVERED (From - To)</b> FY18-FY20	
<b>4. TITLE AND SUBTITLE</b> A Tutorial on the Rapid Distortion Theory Model for Unidirectional, Plane Shearing of Homogeneous Turbulence					<b>5a. CONTRACT NUMBER</b>	
					<b>5b. GRANT NUMBER</b>	
					<b>5c. PROGRAM ELEMENT</b> 611102	
<b>6. AUTHOR(S)</b> Carl R. Hart, Gregory W. Lyons					<b>5d. PROJECT NUMBER</b> AB2	
					<b>5e. TASK NUMBER</b> A1040	
					<b>5f. WORK UNIT NUMBER</b>	
<b>7. PERFORMING ORGANIZATION NAME(S) AND ADDRESS(ES)</b> U.S. Army Engineer Research and Development Center (ERDC) Cold Regions Research and Engineering Laboratory (CRREL) 72 Lyme Road Hanover, NH 03755-1290  U.S. Army Engineer Research and Development Center (ERDC) Information Technology Laboratory (ITL) 3909 Halls Ferry Road Vicksburg, MS 39180					<b>8. PERFORMING ORGANIZATION REPORT NUMBER</b>  ERDC SR-22-2	
<b>9. SPONSORING / MONITORING AGENCY NAME(S) AND ADDRESS(ES)</b> U.S. Army Corps of Engineers Washington, DC 20314-1000					<b>10. SPONSOR/MONITOR'S ACRONYM(S)</b>	
					<b>11. SPONSOR/MONITOR'S REPORT NUMBER(S)</b>	
<b>12. DISTRIBUTION / AVAILABILITY STATEMENT</b> Approved for public release; distribution is unlimited.						
<b>13. SUPPLEMENTARY NOTES</b>						
<b>14. ABSTRACT</b> The theory of near-surface atmospheric wind noise is largely predicated on assuming turbulence is homogeneous and isotropic. For high turbulent wavenumbers, this is a fairly reasonable approximation, though it can introduce non-negligible errors in shear flows. Recent near-surface measurements of atmospheric turbulence suggest that anisotropic turbulence can be adequately modeled by rapid-distortion theory (RDT), which can serve as a natural extension of wind noise theory. Here, a solution for the RDT equations of unidirectional plane shearing of homogeneous turbulence is reproduced. It is assumed that the time-varying velocity spectral tensor can be made stationary by substituting an eddy-lifetime parameter in place of time. General and particular RDT evolution equations for stochastic increments are derived in detail. Analytical solutions for the RDT evolution equation, with and without an effective eddy viscosity, are given. An alternative expression for the eddy-lifetime parameter is shown. The turbulence kinetic energy budget is examined for RDT. Predictions by RDT are shown for velocity (co)variances, one-dimensional streamwise spectra, length scales, and the second invariant of the anisotropy tensor of the moments of velocity. The RDT prediction of the second invariant for the velocity anisotropy tensor is shown to agree better with direct numerical simulations than previously reported.						
<b>15. SUBJECT TERMS</b> Winds, Atmospheric turbulence, Sound--Propagation, Sound--Transmission, Noise, Acoustical engineering						
<b>16. SECURITY CLASSIFICATION OF:</b>			<b>17. LIMITATION OF ABSTRACT</b>	<b>18. NUMBER OF PAGES</b>	<b>19a. NAME OF RESPONSIBLE PERSON</b>	
<b>a. REPORT</b> Unclassified	<b>b. ABSTRACT</b> Unclassified	<b>c. THIS PAGE</b> Unclassified			<b>19b. TELEPHONE NUMBER (include area code)</b>	
			None	42		